The electrochemical degradation of poly(3,4-ethylenedioxythiophene) films electrodeposited from aqueous solutions

Győző G. Láng [a,*], Mária Ujvári [a], Soma Vesztergom [a], Veniamin Kondratiev [b], Jenö Gubicza [c], Krisztina J. Szekeres [a]

[a] Institute of Chemistry, Department of Physical Chemistry&Laboratory of Electrochemistry and Electroanalytical Chemistry, Eötvös Loránd University, Pázmány P. s. 1/A, H-1117 Budapest, Hungary

[b] Chemical Department, St.Petersburg State University, Universitetskii pr. 26, 198504, Russia

[c] Institute of Physics, Department of Materials Physics, Eötvös Loránd University, Pázmány P. s. 1/A, H-1117 Budapest, Hungary

Abstract

In this review, results of recent studies on the electrochemical stability and degradation properties of poly(3,4-ethylenedioxythiophene) films are summarized, with particular emphasis on the structural changes induced by overoxidation and electrochemical degradation. The most important electrodeposition methods for the preparation of PEDOT films in surfactant free aqueous media have also been summarized, and several experimental techniques suitable for monitoring the degradation process have been discussed. Morphological changes in PEDOT films during overoxidation have been analyzed. Overoxidation mechanisms proposed in the literature have been surveyed.

Keywords: PEDOT; overoxidation; voltammetry; electrochemical impedance; scanning electron microscopy; X-ray diffraction; morphology;

1. Introduction

Inherently conducting polymers have been of great interest to scientists since the initial discovery of polymers with metal type conductivities and this is currently one of the most active areas of research in polymer science and engineering. Polymers can be made to conduct if alternating single and double bonds link their respective carbon atoms. Here, electrons can be

* langgyg@chem.elte.hu

introduced via reduction of the polymer chain, or removed via the oxidation of the polymer chain. It is known that demand for electrically conducting polymers as used in the electronics industry has in the past been met by using high loadings of metal or other conductive powders (e.g. Au, Ag, Cu, Ni and graphite) with the polymer matrix [1]. There are, however, a number of disadvantages to this approach, including high cost and deterioration in other properties of the polymer. Consequently, intrinsically conducting organic polymers have attracted great interest due to their very good electrical conductivity and good environmental stability, combining the advantages of organic polymers and the electronic properties of semiconductors.

Conducting polymers are attractive materials for use in a variety of applications that require materials which are both electrically conducting and mechanically compliant, i.e. in energy conversion/storage, optoelectronics, coatings, sensing applications and supplement the quest for powerful yet small/thin and flexible devices. Electronic and electrochemical devices based on organic materials are light emitting diodes, sensors, actuators, organic thin film transistors, solar cells, memory devices, ion-selective electrodes, microelectrode arrays, fuel cells, etc. [2-16]. Obviously, in all these applications the long term stability of the polymer is of particular concern. This stability can be assessed in terms of the property of interest, such as: mechanical elasticity, conductivity, electrochemical activity, etc.

Intrinsically conducting organic polymers such as polyanilines, polypyrroles and polythiophenes have been studied intensively during the last decades. Poly(3,4-ethylenedioxythiophene) [17], often abbreviated as PEDOT, is relatively stable compared to other conducting polymers. The conjugated polymer backbone, consisting of alternating C-C double bonds, provides for π-orbital overlap along the molecule. PEDOT can be doped with many anions, including macromolecular polyanions such as poly(styrene sulfonate) (PSS). Previous studies have shown that PEDOT is highly insoluble in most solvents, electroactive in aqueous solutions [18-20], and exhibits a relatively high conductivity. On the basis of these results, studies have been performed to investigate the electrochemistry of PEDOT in more detail by using voltammetric techniques (in most cases cyclic voltammetry).

It has been found in Refs. [21-25] that at sufficiently positive electrode potentials, degradation of the polymer occurs. That is, when the positive potential limit of the cyclic voltammogram (CV) is extended to the region in which the "overoxidation" of the polymer film takes place, an oxidation peak (without a corresponding reduction peak) appears in the CV.

In Refs. [22,23,24] it has been shown that PEDOT films in modified electrodes undergo structural changes during the overoxidation (degradation) process. The most probable stages involved in the overoxidation/degradation process are: 1) Overoxidation results in stress

generation in the PEDOT film [26]. 2) Formation of cracks due to internal stress. 3) The products of the degradation of the polymer leave the polymer layer. 4) After the formation of the line cracks, the film stress is partially released. 5) The partial delamination of the polymer layer leads to the exposure of the underlying metal substrate to the electrolyte solution.

Apart from the morphological changes, overoxidation can also affect the charge structure of the polymer film. Poly(3,4-ethylenedioxythiophene) is a redox conductive polymer that incorporates counterions from the electrolyte solution to maintain electroneutrality; thus its charging processes involve a detectable counter-ion flux leaving the film [27].

It should be emphasized here that the polymer film still present on the substrate after overoxidation remains electroactive, and its internal structure may be an interesting subject for further studies, since according to literature reports conducting polymers in different overoxidation states show unique features useful for analytical, sensing and biomedical applications [28-31]. For instance, many studies have demonstrated that overoxidized polypyrrole films exhibit molecular-sieve properties, and such films have been used to fabricate glucose, alcohol, hydrazine, and dopamine sensors [29,32-36]. (Over)oxidized PEDOT films were successfully used for sensing perchlorate [37]. According to [38] overoxidized poly(3,4-ethylenedioxythiophene) film-modified screen-printed carbon electrodes exhibited superior sensitivity and selectivity to dopamine. However, the basis for the observed selectivity of overoxidized polymer films is still not entirely clear [24,36,39].

This review summarizes recent studies on the electrochemical stability and degradation properties of poly(3,4-ethylenedioxythiophene) films, with particular emphasis on the structural changes induced by overoxidation and electrochemical degradation. The most important electrodeposition methods for the preparation of PEDOT films in aqueous media have also been summarized, and techniques suitable for monitoring the degradation process have been discussed.

2. The electrochemical synthesis of Poly(3,4-ethylenedioxythiophene)

Poly(3,4-ethylenedioxythiophene) can be synthesized both by electrochemical and chemical methods. A detailed review of the chemical preparation methods can be found in ref. [40]. The electropolymerization of 3,4-ethylenedioxythiophene (EDOT) is usually carried out in organic solvents such as acetonitrile [41-,,,45] or propylene carbonate [42,46] due to the low solubility of the monomer in water. Nevertheless, since organic solvents are often harmful to health and uneconomical compared to water, there is a growing interest in the

electropolymerization of PEDOT films in aqueous media. This is sometimes achieved by the application of surfactants that can prevent the aggregation of EDOT molecules in aqueous solutions. The most often used surfactants are poly(sodium 4-styrenesulphonate) (NaPSS) and sodium dodecyl sulphate (SDS), however the electrodeposition of PEDOT films may also be carried out in aqueous media that do not contain any surface active agent, i.e. when the aqueous solution contains only the monomer and an inorganic salt. There are several papers that reported the electropolymerization of PEDOT in absence of any surfactants or macromolecules (in most cases only for comparison of the films prepared with and without surfactant) but only a few of these studies deal specifically with the dependence of the film structure on the deposition methods and parameters [14,18,47-49]. In this section we briefly review some of the most common electrochemical methods that can be used for the deposition of PEDOT in surfactant free aqueous media.

2.1 Deposition in surfactant free aqueous solutions by galvanostatic method

In Refs. [22-25] Au | PEDOT films were prepared from 0.01 $mol \cdot dm^{-3}$ ethylenedioxythiophene (EDOT)/0.1 $mol \cdot dm^{-3}$ Na_2SO_4 solution at a constant current density of 0.2 $mA \cdot cm^{-2}$ for 900 s, 1800 s or 7200 s. The thickness of the film can be easily varied by changing the deposition time. The structure of the PEDOT film was globular, cauliflower-like.

Glassy carbon | PEDOT films were synthesized by Zanfrognini et. al. [50] from a 0.01 M EDOT / 0.1 M $LiClO_4$ solution by applying a constant current density of 0.4 $mA \cdot cm^{-2}$ for 20 s. The chronopotentiogram exhibited a maximum potential of +0.92 V, later the potential was stable around +0.90 V vs. Ag / AgCl / 3 M KCl reference.

King et. al. [47] deposited PEDOT on different substrates (Au and Pd sputtered glass, as well as ITO on glass and Pt/Ir balls) and in the presence of various counter-ions. Their method involved a galvanostatic electrolysis at a current density of 0.5 mA/cm^2 for 12 min from solutions containing 0.01 M EDOT and 0.01 M of the studied counter-ion. They characterized the structure of PEDOT films deposited from aqueous poly(styrene sulfonate), chloride, perchlorate, PBS: phosphate buffered solution containing 0.001 M KH_2PO_4, 0.15 M NaCl and 0.0057 M Na_2HPO_4, *para*-toluenesulfonate, heparin, glutamate, hyaluronic acid, bovine serum albumine, poly(*d*-lysine), and biotin solutions, and found that the selection of counter-ions for PEDOT deposition affects both the electrical properties and the morphology of the obtained film.

Bobacka et. al. [14,18] described the galvanostatic deposition of PEDOT on glassy carbon [14] and Pt [18]. They used a solution that contained 0.01 M EDOT and 0.1 M

supporting electrolyte (either KCl, NaCl or NaPSS with an average molar mass of 7000). The auxiliary electrode was a glassy carbon rod in both cases and the reference electrode was either Hg / Hg_2Cl_2 / 3 M KCl [14] or Ag / AgCl / 3 M KCl [18]. The applied current density was 0.2 mA/cm^2, the deposition time has been varied between 71 and 1071 s.

2.2 Deposition in surfactant free aqueous solutions by potentiostatic method

Du and Wang [51] prepared PEDOT by potentiostatic deposition on a Pt disk (⌀ = 2 mm) from a 0.01M EDOT + 0.1 M $LiClO_4$ aqueous solution. The same charges (0.2 C) were passed at the different synthesis potentials and the hydrodynamic conditions were maintained by constant stirring. The potential was varied between 0.8 and 1.5 V vs. KCl-saturated calomel electrode (SCE). The capacitance of the produced film exhibited a minimum, while the film resistance and the deposition time (i.e., the time required for the passing of 0.2 C charge) exhibited a maximum at 1.2 V. Over 1.1 V deposition potential overoxidation of PEDOT takes place parallel to the EDOT oxidation.

Pigani et al. [52] followed the electropolymerization of PEDOT on gold by EQCM and spectroelectrochemistry. Potentiostatic electrolysis lasted 360 s in 3 mM aqueous EDOT solution containing 0.3 M $LiClO_4$ as supporting electrolyte. The applied potentials (0.75 V, 0.80 V, 0.85 V and 0.90 V vs. Ag / AgCl / 3 M KCl) were chosen carefully in order to avoid the over-oxidation of the formed polymer. At 0.75 V, no frequency change was detected with the EQCM, indicating that no deposition occurred at this potential. At potentials more positive than 0.80 V, the higher the applied potential the higher the frequency change.

Ventosa et al. [53] investigated the oligomers occluded in electrochemically synthesized PEDOT. The films were grown on different substrates potentiostatically by applying an anodic potential of +1.00 V vs. Ag / AgCl / KCl (3 M) for 250 s in 0.003 M EDOT + 0.2 M $LiClO_4$ aqueous solution. Both spectroelectrochemical and scanning electrochemical microscopy measurements showed that oligomer release took place from −0.30 V downwards in a 0.2 M $LiClO_4$ solution. From the mass spectroscopy results it can be concluded that the most stable oligomeric forms are the tetramer and the hexamer and only traces of the longest oligomeric compounds are released to solution.

Lupu et. al. [54] deposited PEDOT by potentiostatic method and by using sinusoid voltage perturbation from 0.01 M EDOT and 0.1 M $LiClO_4$ containing solution at fixed DC potential 0.95 V vs. SCE reference electrode for 300 s. The amplitudes of the applied AC perturbations were 5 and 50 mV. In case of the 5 mV perturbation the properties of the film were similar to those of PEDOT prepared by a regular potentiostatic method. In case of 50 mV

amplitude the porosity of the film became higher. The advantage of the sinusoidal method is that it allows the estimation of electrochemical parameters, such as charge transfer resistance and exchange current during the polymerization process.

2.3 Deposition in surfactant free aqueous solutions by potentiodynamic method

Zhou et. al. [55] deposited PEDOT on ITO by using a potentiodynamic method (cyclic voltammetry) from 0.1 M KNO_3 + 0.01 M EDOT solution in different potential ranges. The lower limit of the CVs was 0.4 V (vs. SCE), the final charge density was 0.17 C/cm^2. The structure of the film changed with increasing the high potential limit: the globules grew larger and many globules became well separated, leading to an increased roughness. The capacitance of films prepared with the application of a high potential limit of 1.4 V was less than that of films polymerized with upper potential limit of both 1.05 and 1.2 V. These findings are related to the overoxidation of the PEDOT films. The microstructure – which is based on nanosheets – does not change with increasing oxidation limit.

Nasybulin et. al. [48] investigated the effect of the solubilizing agent during potentiodynamic and potentiostatic deposition. The plater solution contained 10.0 mM EDOT, 0.5 M $NaNO_3$ and different solubilizing agents. The voltammetric curves ran from 0.0 V to 1.0 V (vs. Ag/AgCl/3 M NaCl) at 100 mV/s polarization speed, potentiostatic deposition was performed at 1.0 V (up to charge density 6.25 mC/cm^2). It was concluded that anodic solubilizing agents favor polymerization by lowering the oxidation potential of EDOT and by eliminating the induction period. The formed films demonstrated longer conjugation length, higher transparency and increased conductivity. Cationic surfactants increased the oxidation potential and exhibited slow polarization kinetics.

3. The electrochemical characterization of overoxidized PEDOT

3.1 Cyclic voltammetry

As mentioned in the introduction cyclic voltammetry (CV) is a useful tool for the investigation of the electrochemistry of PEDOT. It has been found that when the positive potential limit of the CV is extended into the region in which the overoxidation of the polymer film takes place, an oxidation peak (without a corresponding reduction peak) appears [21], but only minor changes can be observed in the properties of the cyclic voltammograms recorded in the "stability region" before and after overoxidation. The influence of the electropolymerisation potential on the properties of PEDOT films obtained in aqueous solutions has been studied in

[51,52]. It has been concluded in [55] that strong overoxidation of PEDOT takes place when the electropolymerisation potential is more positive than +1.10 V vs. SCE, and the extent of overoxidation is smaller when the potential ranges from +0.80 to +1.10 V.

Overoxidation of PEDOT films prepared electrochemically under "normal" conditions has been investigated in [22-25]. A series of cyclic voltammetric curves of Au|PEDOT|0.1 M sulfuric acid (aq.) and Pt|PEDOT|0.1 M sulfuric acid (aq.) electrodes at different sweep rates (v = 10, 20, 50, 100 mVs^{-1}) are shown in Fig. 1 (geometric surface area: 2.0 cm^2). The rectangular nature of the CV curves indicates capacitive behavior of the electrodes (Fig. 1a and Fig. 1b). The charge associated with the charging/discharging process is approximately the same for both electrodes [23], i.e. between –0.3 and 0.8 V vs. KCl-saturated calomel electrode (SCE) the oxidation-reduction process of the PEDOT films is reversible.

According to published results [22], irreversible oxidation of the PEDOT film starts at or above 0.8 V vs. SCE. This means that at potentials more positive than 0.8 V vs. SCE irreversible degradation of the polymer layer occurs as it can be seen in Fig. 2, where a series of cyclic voltammetric curves recorded for Au|PEDOT|0.1 M sulfuric acid (aq.) (Fig. 2a) and Pt|PEDOT|0.1 M sulfuric acid (aq.) (Fig. 2b) electrodes at a sweep rate of v = 50 mV s^{-1} are presented [23]. The potential programs applied to the electrodes are given in the inserts. After "moderate" overoxidation (up to 1.2 V vs. SCE) there are only small differences between the voltammograms recorded in the −0.3 V to 0.8 V ("narrow") potential range before and after overoxidation (curves 1 and 5 in Figs. 2a and 2b).

Both in the cases of Au|PEDOT and Pt|PEDOT the cyclic voltammograms change considerably if the positive limit of the electrode potential is extended to 1.5 V vs. SCE ("strong" overoxidation, curves 2-4 in Fig. 3a and 3b). In case of Au|PEDOT a broad oxidation peak at about 1.30-1.35 V with no corresponding reduction peak can be observed in the first cycle. The voltammetric behavior of Pt|PEDOT in the potential range of -0.3 to 1.5 V vs. SCE is similar to that of Au|PEDOT, however, no distinct peak appears on the voltammograms. As it can be seen from Figs. 3a and 3b, the effects of overoxidation on the oxidation current are common for both electrodes: the peak current decreases with the number of scanning cycles (curves 2-4). This rapid decrease of the oxidation current with the number of cycles and the absence of the reduction peak suggest that the oxidation process lead to irreversible changes in the polymer film. Indeed, the cyclic voltammograms recorded before and after overoxidation (curves 1 and 5 in Figs. 3a and 3b) are similar in shape and show typical capacitive behavior at

the narrow voltage window (−0.3 V to 0.8 V vs. SCE), but the redox capacity of the (over)oxidized polymer film is considerably smaller than that of the freshly prepared film.

3.2 Impedance measurements

The theory of the impedance method for an electrode with diffusion restricted to a thin layer is well established [56], however, in the case of polymer-modified electrodes the 'ideal' response, i.e., a separate Randles circuit behavior at high frequencies, a Warburg section at intermediate frequencies, and a purely capacitive behavior due to the redox capacitance at low frequencies (see Fig. 4) can rarely be observed.

Unfortunately, there are no studies in the literature dealing directly with the impedance of overoxidized PEDOT films, only some tentative or qualitative interpretations of such impedance spectra can be found in a few recent studies [22,23,25]. For instance, impedance spectra of freshly prepared and overoxidized Au/PEDOT in 0.5 M H_2SO_4 solution are presented in [22] (see Figs. 5 and 6). The impedances of freshly prepared electrodes at medium and low frequencies (ω < 50 Hz) can be well approximated in terms of a constant phase element (CPE):

$$Z(\omega) = R_u + \frac{1}{B}(i\omega)^{-\alpha}, \qquad (1)$$

where ω is the angular frequency, R_u is the uncompensated ohmic resistance, B and α are the CPE parameters, and i is the imaginary unit. The values of α are close to unity. (It should be noted that at higher frequencies a small arc can be identified which can be observed more clearly in the spectra recorded after overoxidation, i.e. after repetitive cycling of the electrode potential between –0.3 and 1.5 V vs. SCE. On the other hand, it has been found that for thin PEDOT films in very clean solutions the CPE parameter α is close to unity which indicates a nearly perfect capacitive behavior. However, for thicker films, this value is always smaller [23,25]. These issues should be addressed in future studies.)

In Fig. 5 impedance spectra (complex plane plots) of freshly prepared Au/PEDOT in 0.5 M H_2SO_4 solution at different electrode potentials are shown ($t_f \approx 0.7$ μm, geometric area ≈ 1 cm^2). In the frequency range 0.1 Hz – 10 kHz and at electrode potentials ranging from 0.1 V to 0.7 V vs. SCE the impedance spectra indicate an almost purely capacitive behavior (the "low frequency capacity" of the film is $C_L \approx 2.9$ mF·cm^{-2} at 0.1 V vs. SCE and $C_L \approx 2.7$ mF·cm^{-2} at 0.4 V vs. SCE). However, at electrode potentials E > 0.7 V vs. SCE the "arc" indicates that an interfacial charge transfer process, which can most probably be attributed to the slow degradation of the PEDOT film, has become fast enough to be observed (see the insert in Fig. 5).

As it can be seen from Fig. 6, the impedance spectra of overoxidized PEDOT on gold differ from those measured for freshly prepared Au/PEDOT. The film was oxidized by cycling the potential between -0.4 V and 1.5 V vs. SCE. The most interesting feature is the appearance of an arc (or a "depressed semicircle") at high frequencies in the complex plane impedance plot. The "low frequency capacity" of the degraded film is about 2 $mF \cdot cm^{-2}$ at 0.35 V vs. SCE. The increase of the charge transfer resistance with the level of degradation is in accordance with the results for polypyrrole on Pt published in [57]. The decreasing capacitance and the increasing charge transfer resistance suggest that during overoxidation the electrochemical activity of the film decreases and the charge transfer process at the metal/film interface becomes more hindered than in the case of pristine films.

3.3 Electrochemical-mechanical properties

According to experimental results, the mechanical properties of conductive polymers may change significantly during oxidation or reduction processes [58,59]. Considerable stress changes in dodecylbenzenesulfonate-doped polypyrrole films have been detected by using a micromechanical cantilever-based sensor [60]. In these experiments the polymer was electrochemically switched between its oxidized and neutral state by cyclic voltammetry.

The "electrochemical bending beam" ("bending cantilever") method [61-69] can be effectively used in electrochemical-mechanical experiments, since the changes of the stress (g_f) in a thin film or other conducting layer on one side of an insulator (e.g. glass) strip (cantilever) in contact with an electrolyte solution can be estimated from the changes of the radius of curvature of the strip. If the potential of the electrode changes, electrochemical processes resulting in the change of g_f induces a bending moment and the strip bends. The change of g_f can be obtained by an expression based on a generalized form of Stoney's equation [70,26,61]

$$\Delta g_f = k_i \Delta(1/R) \tag{2}$$

where k_i depends on the design of the electrode. The change in the curvature of the cantilever, $\Delta(1/R) = \Delta g_f / k_i$, can be calculated, if the changes of the deflection angle $\Delta\theta$ of a laser beam mirrored by the metal layer on the plate are measured using an appropriate experimental setup. For the geometry shown in Fig. 7, the following approximate equation can be derived for large R and s, and small θ [61,71-73]:

$$\Delta\left(\frac{1}{R}\right) \approx \frac{\Delta\theta}{2n_{s,a}h} \approx \frac{\Delta b}{2n_{s,a}hl}, \tag{3}$$

where h is the distance between the level of the solution in the cell and the reflection point of the laser beam (measured e.g. with the help of a cathetometer); l is the distance between the electrode and the position sensitive photo detector (PSD), Δb is the change of the position of the light spot on the PSD, and $n_{s,a}$ is the refractive index of the solution with respect to air.

As discussed in the previous sections, between –0.3 and 0.8 V vs. SCE the oxidation-reduction process of the PEDOT films is reversible, but at potentials $E > 0.8$ V vs. SCE irreversible degradation of the polymer layer occurs. In ref. [25] a series of voltdeflectograms ($\Delta(1/R)$ vs. E curves) has been recorded for a Au | PEDOT | 0.1 M sulfuric acid (aq.) electrode (geometric surface area: 4.0 cm^2) at a sweep rate of $v = 50$ mV s^{-1}. Some of these curves are shown in Fig. 8b. The potential program applied to the electrode is given in Fig. 8a. The corresponding voltammograms showed capacitive behavior if the potential limit is kept below 0.8 V. If the polarization potential exceeded this critical value an oxidation peek without corresponding reduction peek appeared ("overoxidation cycles"). The shapes of the $\Delta(1/R)$ vs. E curves before and after moderate oxidation were similar, but the change in $1/R$ (between minimum and maximum) was slightly greater in the case of the pristine film.

After extending the positive potential limit up to 1.5 V vs. NaCl-saturated calomel electrode (SSCE), the shape of the $(1/R)$ vs. E curves changed dramatically (curves 6–7 in Fig. 2) and begins to resemble more and more that of the $(1/R)$ vs. E curve for bare Au [22,23,26].

Voltdeflectograms for the Pt | PEDOT | 0.1 M sulfuric acid (aq) electrode can be found in ref. [23].

4. SEM micrographs and X-ray diffractograms of the overoxidized PEDOT layers

SEM images together with X-ray diffractograms of PEDOT films freshly prepared on gold are presented in refs. [24,25]. One can see in the image detected by secondary electrons (SE), that well-separated globules (or cauliflower-like particles) are present on the top of the polymer layer (Fig. 9b, see also refs. [22,23]). The backscattered electron (BSE) micrograph taken from the same area (which characterizes a thicker layer compared to SE) shows that the globules are attached to an underlying smoother polymer layer (Fig. 9c). The X-ray diffraction pattern indicates that the as-prepared sample is amorphous (Fig. 9a).

In Fig. 10 X-ray diffractogram and SEM images of the polymer film after moderate overoxidation (after the completion of 3 potential cycles up to 1.2 V vs. SSCE) can be seen. The XRD spectrum is still characteristic for amorphous state but small peaks appear as sign of

crystalline phase. The most striking difference between the micrograph shown in Fig. 10b and that of the freshly prepared sample in Fig. 9b is the appearance of narrow cracks or crevices in the SEM image of the oxidized film. The cracks resulted in bright spots ("islands") in the backscattered SEM image (Fig. 10c).

After further oxidation the XRD peaks corresponding to the crystalline polymer are growing (Fig. 11a), the SEM images show interconnected crevices (Figs. 11b-c).

After strong overoxidation (i.e. after the completion of 3 potential cycles up to 1.5 V vs. SSCE) well-separated X-ray diffraction peaks can be observed (Fig. 12a). The diffraction peaks of crystalline PEDOT were indexed according to previous studies [74,75]. These works identified this phase as orthorhombic structure. According to Figs. 10a, 11a and 12a the diffraction peaks of PEDOT became sharper and more intensive due to the electrochemical treatment. This indicates that besides the degradation of the PEDOT film its crystallinity was gradually improved with increasing the number of oxidation cycles. In the SEM micrographs the cauliflower-like structure is still present, but the film forms islands on the surface of the substrate. The width of the crevices shown in Fig. 12b is about 2-3 μm [25]. According to the backscattered SEM micrographs (Fig. 12c) the crevices form a widespread network. EDX analysis proved that only Au is present at the bottom of the grooves [22-25].

5. The suggested overoxidation mechanism of PEDOT

Despite of its deep impact on the life expectancy of (opto)-electronic devices, the number of mechanistic studies dealing with the anodic degradation of PEDOT is very limited. Nevertheless, the oxidative degradation of polythiophenes in general was relatively widely studied, and this may provide an insight into the over-oxidation mechanism of PEDOT as well.

Electrochemical studies accompanied by electron microprobe analysis as well as NMR and IR spectroscopic surveys [76] revealed that the first (reversible) stage of anodic polythiophene oxidation is often accompanied by the substitution of nucleophiles on the 3rd or 4th position of the thiophene units (Figure 13). The nucleophiles are either solvents or counter ions (e.g., water, hydroxide, methanol or halides); the resulting polymers are still conductive and electroactive, with a new optical gap induced by the substitution [77,78].

By further (over-)oxidation, polythiophenes are irreversibly transformed to a non-conducting state [79]. At electrode potentials ranging from 1.8 to 2.2 V vs. SCE, the voltammograms of polythiophene films in contact with wet acetonitrile solutions exhibit an irreversible anodic peak. A study of Beck and Barsch [80] revealed by IR spectroscopy that at

this potential range the thiophenic sulphur of polythiophene is sulphonated, resulting in the formation of SO_2 groups. According to the scenario proposed by these authors (Figure 14) the partial over-oxidation is followed by an oxidative SO_2 elimination and the formation of carbonyl groups at the 2nd, 3rd and 5th positions on the thiophene rings. The electrical conductivity of the polythiophene film concomitantly decreases due to an interruption of conjugation routes by the formed carbonyl groups. Further over-oxidation leads to the cleavage of C—C bonds and the formation of terminal carboxylic groups.

Tehrani *et al.* [78] suggested that the above mechanism describing the overoxidation of polythiophenes *in general* should also be valid for the case of PEDOT *in particular*. They investigated the structural changes of PEDOT:PSS films using Fourier-transformed infrared and X-ray photoelectron spectroscopy, and have pointed out significant differences between the spectra of pristine and over-oxidized PEDOT:PSS. While at pristine films they only detected the usual strong absorption at high wave numbers due to the extended π-conjugation, their spectra obtained from over-oxidized films exhibited other absorption bands as well, which they assigned to SO_2, C=O and (carboxylic) OH groups formed upon over-oxidation. Based on these results it was hypothesised [78] that the presence of ethylene-dioxy groups does not create fundamental differences between the overoxidation mechanism of PEDOT and the scenario described by Barsch and Beck [80] for polythiophene. By means of linear sweep voltammetry, it has also been confirmed [78] that the anodic onset potential of the over-oxidation of PEDOT depends strongly on the pH. At pH > 10 where the amount of OH^- ions in the electrolyte becomes more significant, PEDOT films are more easily overoxidized than at more acidic pH values [78]. This indicates that the amount of counter ions (nucleophiles) in the studied medium may also have a significant role in the over-oxidation process.

It should be noted that the degradation of PEDOT films as a result of non-electrochemical effects was also studied. For example, it was pointed out by Crispin *et al.* [81,82] that ultraviolet light radiation can induce photo-oxidation which may reduce the conjugation length in the polymer chains due to the formation of sulphone groups and chain scission accompanied by the addition of carbonyl or carboxylic groups. The spectral sensitivity of PEDOT:PSS films was also studied in a recent work of Elschner [83]. It was shown that exposing the films to light of wavelength $\lambda = 315$ nm has to be strictly avoided in order to maintain the film's sheet resistance; and that the degradation can be significantly slowed down by using proper encapsulation, e.g., between two glass plates. Elschner argued that the oxidation should occur at the sulphur atom of the thiophene ring or at terminating segments. The former

process may interrupt the conjugation within the polymer chains, thereby reducing the overall conductivity of the film.

A similar chemistry may be held responsible for the thermal degradation of PEDOT in air [84]. Upon exposure to air, the conductivity of PEDOT thin layers doped with iron(III) tris-p-toluenesulfonate was found to decay roughly according to first order kinetics, with rate constants obeying the Arrhenius law at the approximate temperature range of 100 to 150 °C [85].

6. Concluding remarks

The experimental results reviewed above support the mechanistic picture, according to which in PEDOT-modified electrodes, the originally compact and strongly adherent PEDOT films undergo structural changes during electrochemical degradation, and agree with earlier observations that the porosity of the film increases progressively during the degradation process. Apparently, the formation of quite well-ordered arrays of islands and trench-like structures is a common occurrence during overoxidation of PEDOT layers. In the XRD patterns, the diffraction peaks became sharper and more intensive during the subsequent oxidation cycles indicating an increase in the degree of crystallinity of the polymer. The charge transfer process at the metal/film interface is somewhat more hindered in case of the degraded film most probably due to the partial delamination of the polymer film from the underlying metal. The results also suggest that, besides the increase in the porosity, the generation of sites with novel catalytic and binding properties may also influence the sensitivity and specificity of conducting polymer-based sensors for the analysis of organic and inorganic substances.

Acknowledgements

Financial support from the Hungarian Scientific Research Fund (grants No. K 109036) and from the Russian Foundation for Basic Research (grant N-13-03-00984) are gratefully acknowledged.

Figures

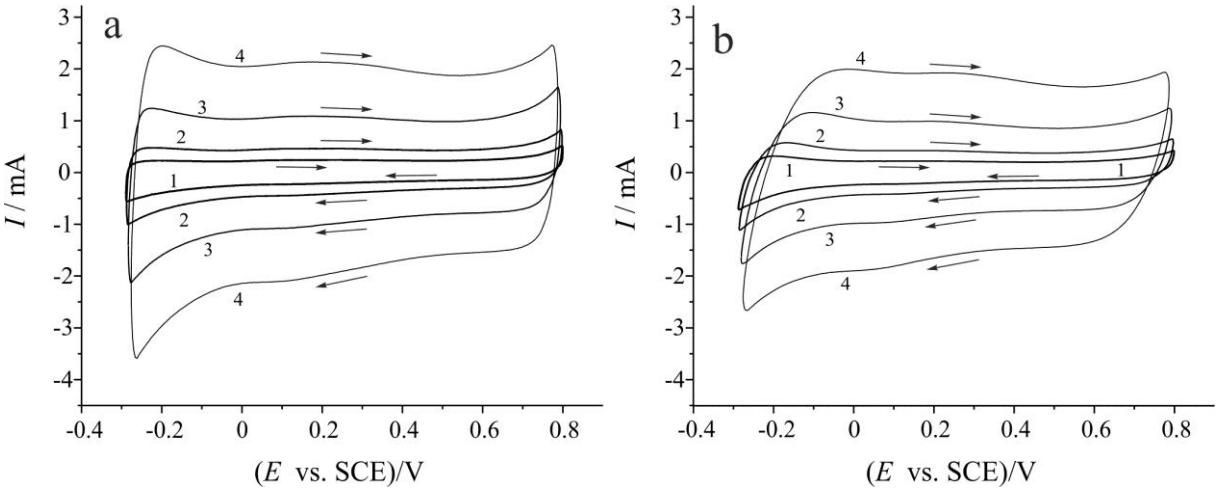

Figure 1

Cyclic voltammograms of PEDOT films electrodeposited on gold-on-glass (a) and platinum-on-glass strips (b) recorded in $c = 0.1$ mol·dm^{-3} H_2SO_4 solution at different sweep rates. 1: $v = 10$ mVs^{-1}; 2: $v = 20$ mVs^{-1}; 3: $v = 50$ mVs^{-1}; 4: $v = 100$ mVs^{-1}; Geometric electrode area: 2.0 cm^2. *E*: electrode potential, *I*: current. Adapted from [23].

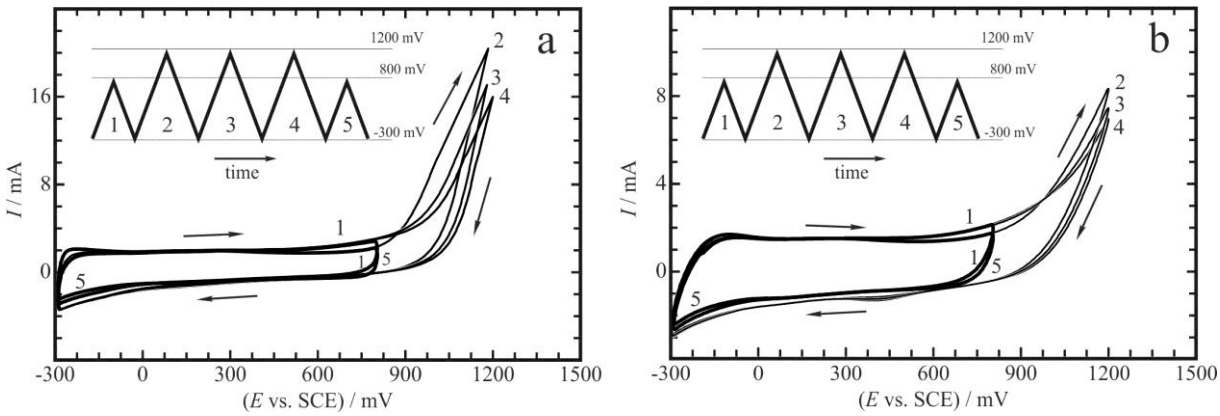

Figure 2

The series of cyclic voltammetric curves recorded according to the potential programs indicated by the saw-tooth like inserts (sweep rate: $v = 50$ mV s^{-1}). One "narrow-range" CV (curve 1) taken immediately before and one (curve 5) taken immediately after the 3 cycles (curves 2-4) recorded in the potential range -300 mV vs. SCE – 1200 mV vs. SCE are presented. a: Au | PEDOT | 0.1 M sulfuric acid (aq.); b: Pt | PEDOT | 0.1 M sulfuric acid (aq.). Geometric electrode area: 2.0 cm^2. *E*: electrode potential, *I*: current. Adapted from [23].

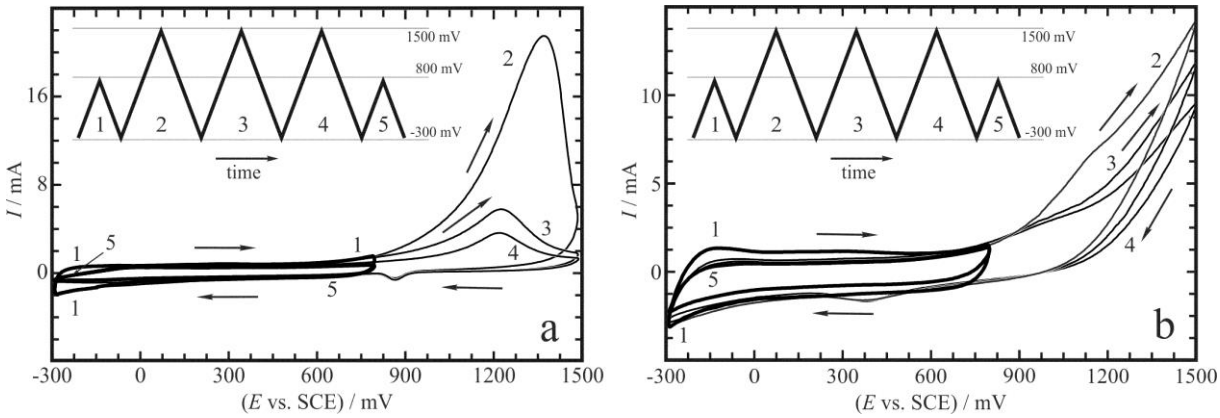

Figure 3

The series of cyclic voltammetric curves recorded according to the potential programs indicated by the inserts (sweep rate: $v = 50$ mV s^{-1}). One "narrow-range" CV (curve 1) taken immediately before and one (curve 5) taken immediately after the 3 "wide-range" cycles (curves 2-4, potential range -300 mV vs. SCE – 1500 mV vs. SCE) are presented. a: Au | PEDOT | 0.1 M sulfuric acid (aq.); b: Pt | PEDOT | 0.1 M sulfuric acid (aq.). Geometric electrode area: 2.0 cm^2. *E*: electrode potential, *I*: current. Adapted from [23].

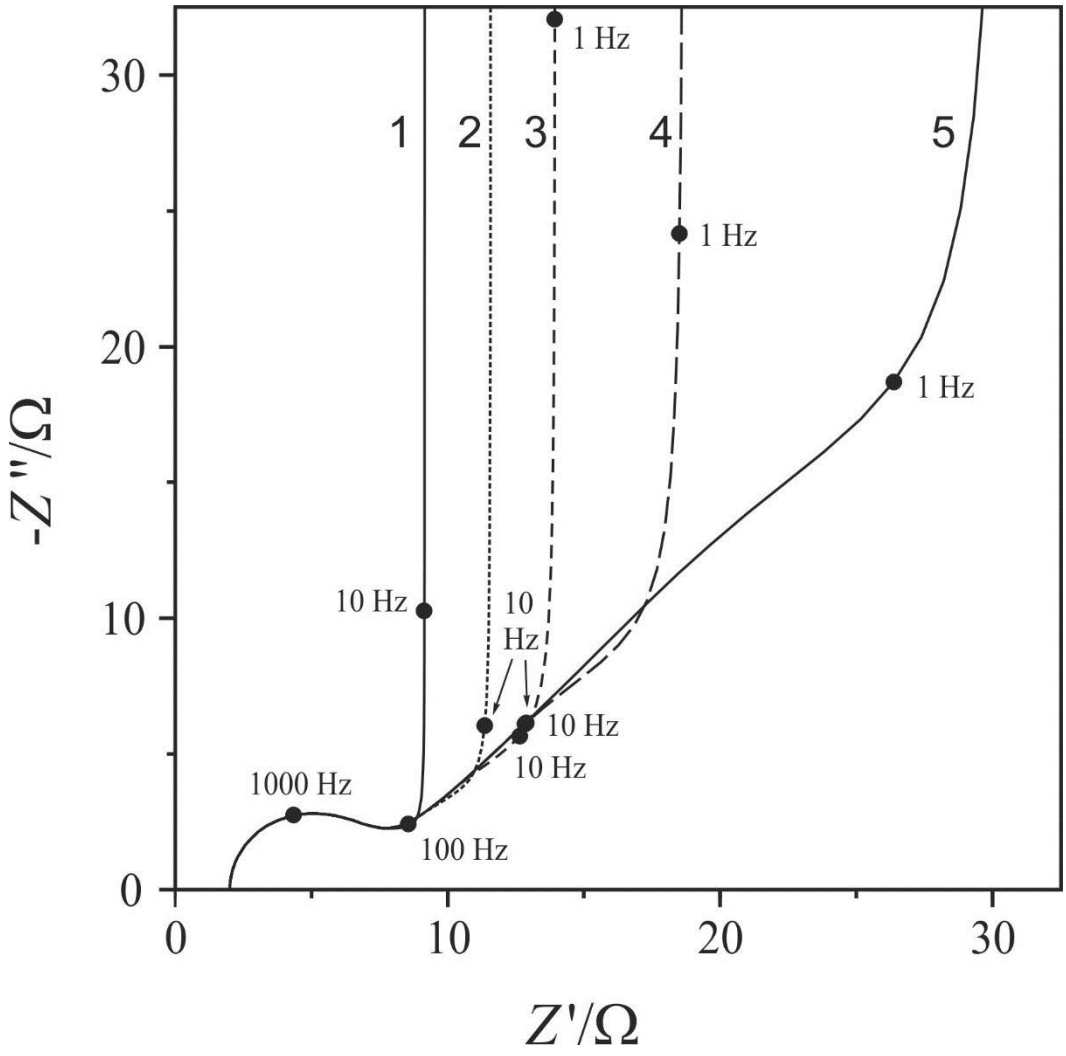

Figure 4

The complex-plane impedance plot representation (also called Argand diagram or Nyquist diagram) of the 'ideal' impedance spectra of polymer-modified electrodes in the case of reflective boundary conditions. Effect of the ratio of the film thickness (L) and the diffusion coefficient (D), $L / D^{½}$: (1) 0.1; (2) 0.2; (3) 0.3; (4) 0.5 and (5) 1 $s^{½}$. Ohmic resistance, R_{Ω} = 2 Ω; charge transfer resistance, R_{ct} = 5 Ω; Warburg coefficient, σ = 50 Ω $s^{-½}$; double layer capacitance, C_{dl} = 20 μF. The smaller numbers refer to values of frequency. Adapted from [56].

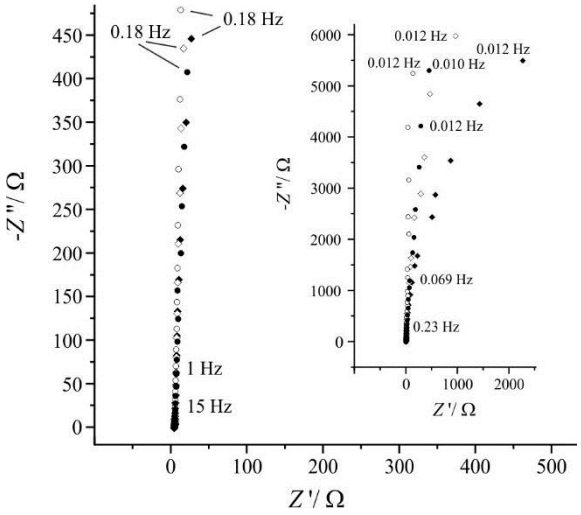

Figure 5

Impedance spectra (complex plane plots) of freshly prepared Au/PEDOT in 0.5 M H_2SO_4 solution at different electrode potentials. •: E = 0.10 V vs. SCE; ○: E = 0.40 V vs. SCE; ◊: E = 0.70 V vs. SCE; ♦: E = 0.80 V vs. SCE; Adapted from [22].

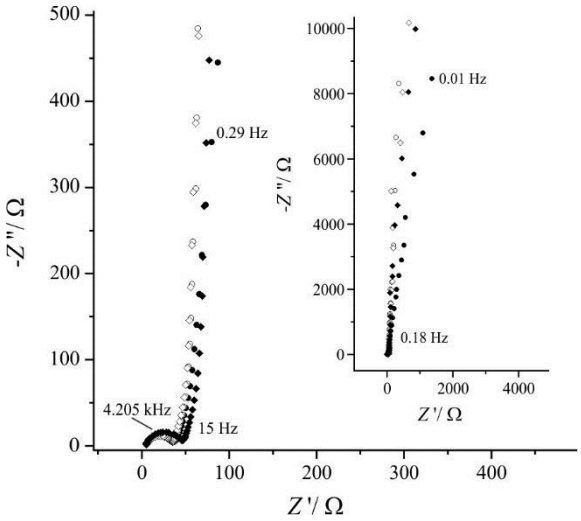

Figure 6

Impedance spectra of the overoxidized Au/PEDOT film in 0.5 M H_2SO_4 solution at different electrode potentials. •: E = 0.05 V vs. SCE; ○: E = 0.35 V vs. SCE; ◊: E = 0.50 V vs. SCE; ♦: E = 0.65 V vs. SCE; Adapted from [22].

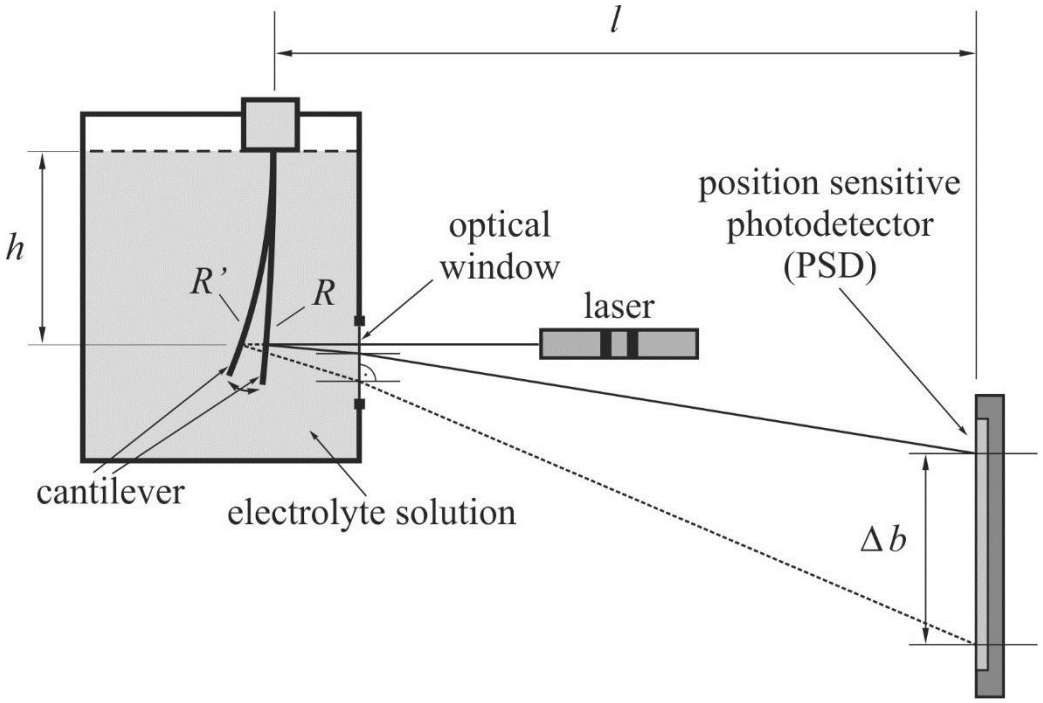

Figure 7

Scheme of the electrochemical (optical) bending beam setup. Δ*b*: displacement of the light spot on the position sensitive detector if the radius of curvature changes from *R* to *R*'; *l*: the distance between the electrode and the position sensitive photodetector (PSD); *h*: the distance between the solution level and the reflection point.

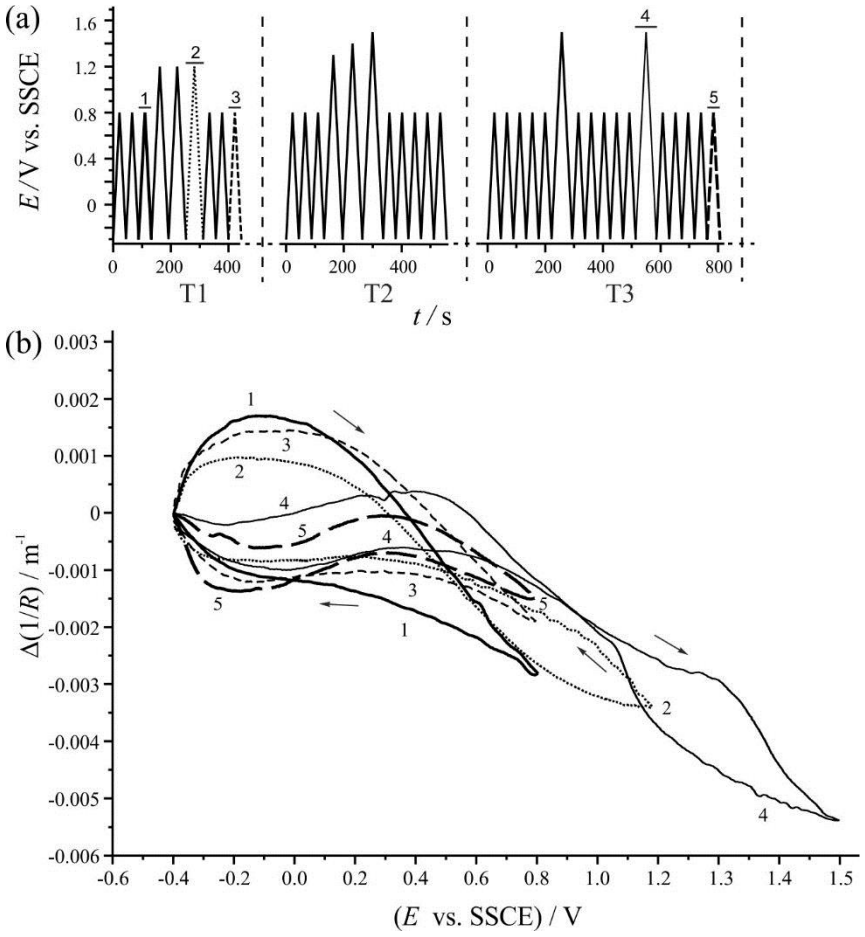

Figure 8

(a) The potential program applied to the Au | PEDOT | 0.1 M sulphuric acid electrode. Sweep rate: $v = 50$ mV s^{-1}.

(b) The voltdeflectograms recorded in time intervals "1" - "5" (see Fig. 8a). *E*: electrode potential, *R*: radius of curvature of the cantilever (Film thickness: $d \approx 1.4$ µm). Adapted from [23 and 25].

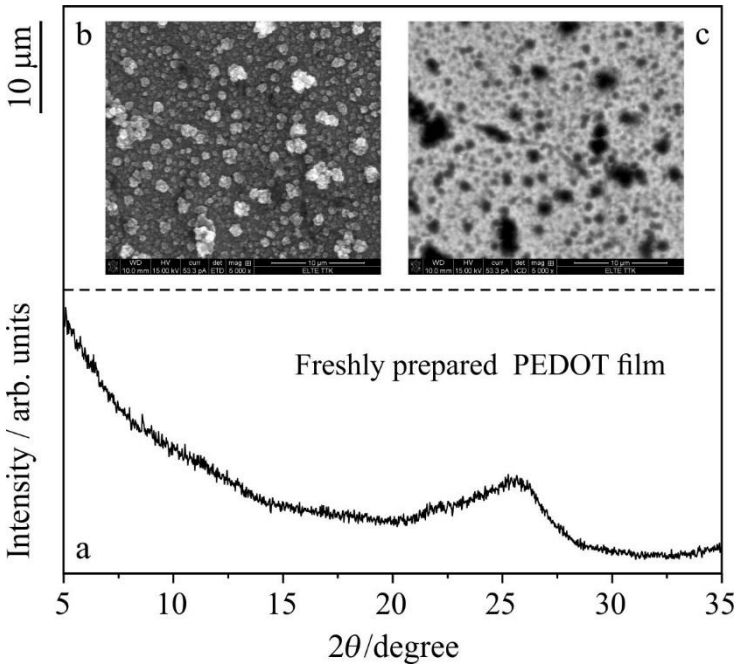

Figure 9

Structure of the freshly prepared PEDOT film. (a): X-ray diffractogram. (b) Secondary electron SEM image. (c): The corresponding backscattered SEM image taken from the same area. The length of the vertical black bar left to the images corresponds to 10 µm. Adapted from [25].

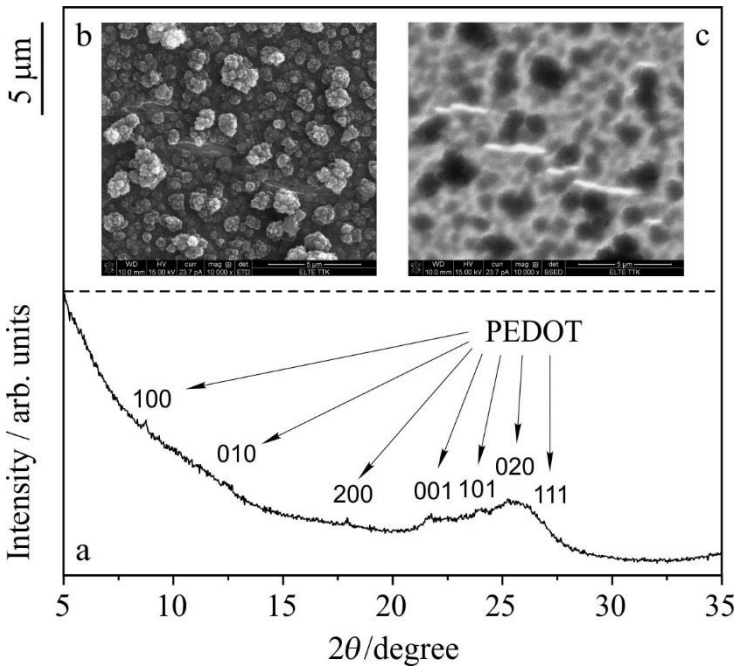

Figure 10

Structure of the oxidized PEDOT film after after moderate overoxidation (X-ray diffractogram and SEM micrographs recorded at the end of time interval "T1" in Fig. 8a, i.e.

after the completion of 3 potential cycles up to 1.2 V vs. SSCE). (a): X-ray diffractogram. (b) Secondary electron SEM image. (c): The corresponding backscattered SEM image taken from the same area. The length of the vertical black bar left to the images corresponds to 5 µm. Adapted from [25].

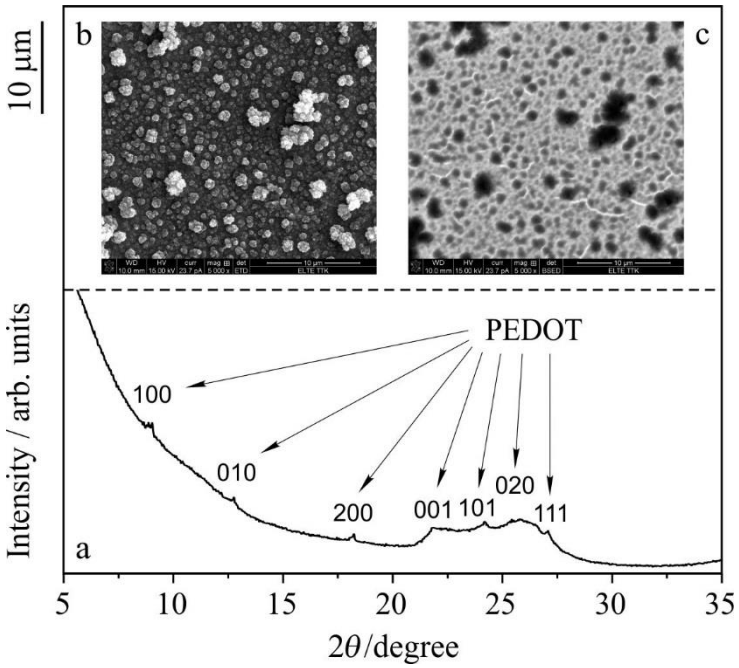

Figure 11

Structure of the oxidized PEDOT film at the end of time interval "T2" in Fig. 8a. (a): X-ray diffractogram. (b) Secondary electron SEM image. (c): The corresponding backscattered SEM image taken from the same area. The length of the vertical black bar left to the images corresponds to 10 µm. Adapted from [25].

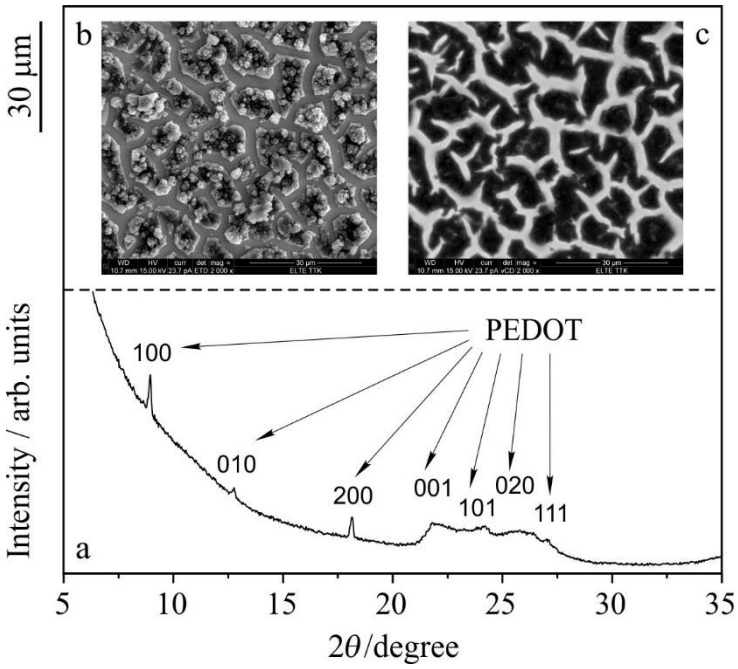

Figure 12

Structure of the oxidized PEDOT film after strong overoxidation (X-ray diffractogram and SEM micrographs recorded at the end of time interval "T3" in Fig. 8a, i.e. after the completion of 3 potential cycles up to 1.5 V vs. SSCE). (a): X-ray diffractogram. (b) Secondary electron SEM image. (c): The corresponding backscattered SEM image taken from the same area. The length of the vertical black bar left to the images corresponds to 10 µm. Adapted from [25].

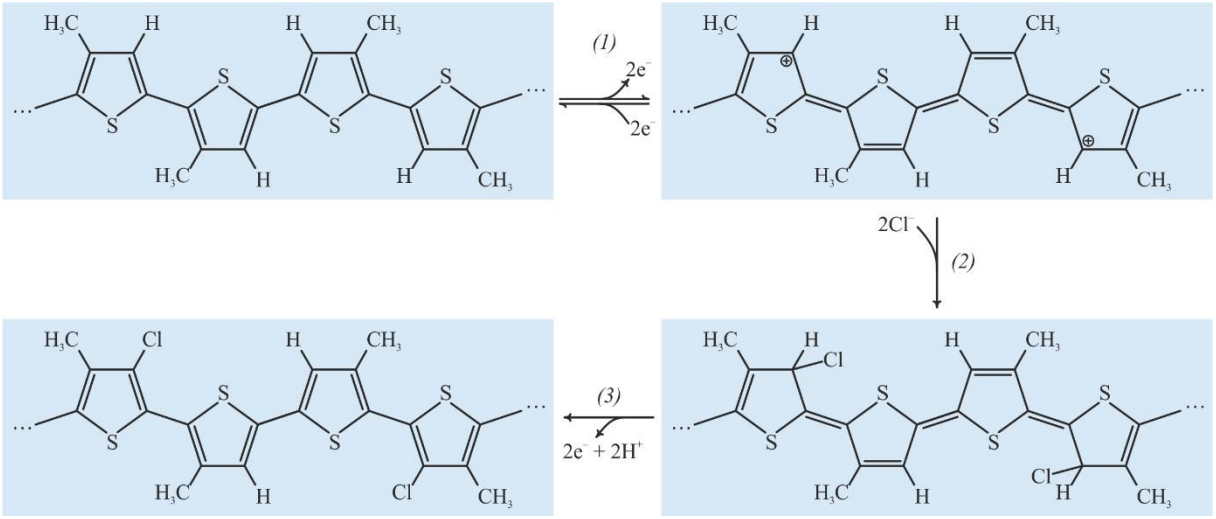

Figure 13

The oxidation of poly(3-methylthiophene) (step *1*) in the presence of chloride results in substitution of the hydrogen at the 4th position of each 3rd thiophene rings by the halide (steps *2* and *3*). Scheme adapted from [76].

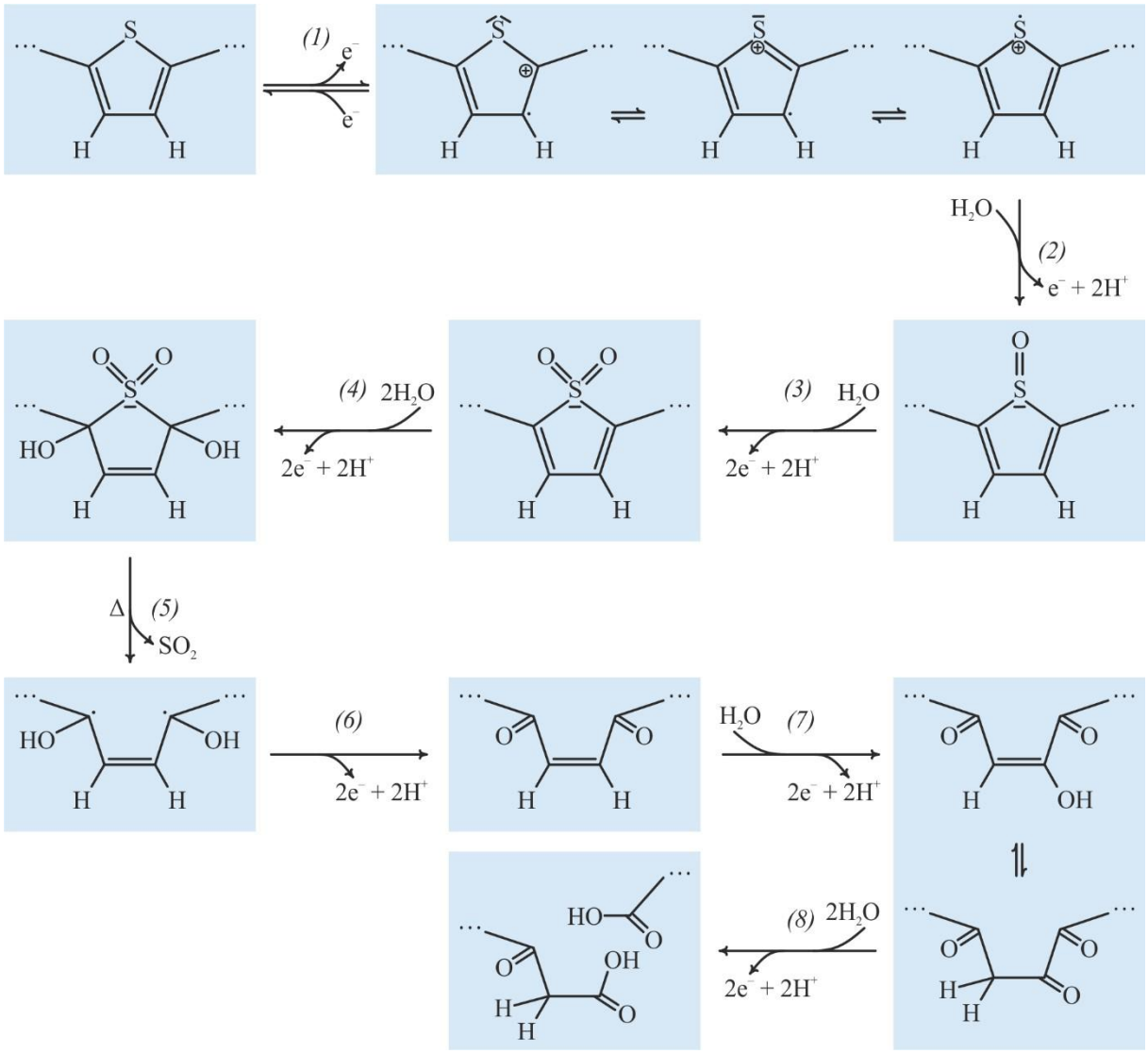

Figure 14

Mechanism of the over-oxidation of polythiophene. Step *1* proceeds reversibly in the course of the redox peak (doping), while steps *2* and *3* are part of the large over-oxidation peak. A sequence of two further $2e^-$ steps, (*4* and *5*) leads then to the elimination of SO_2, initiated by a 2,5-hydroxylation. Thereafter, 2,5-diketones are formed in step *6* and a hydroxylation in the 3-position follows in step *7*. The mesomer of the formed enol yields a vicinal 2,3-diketon, the C—C bond of which is easily cleaved in the last anodic step (*8*) to yield two carboxylic groups. Altogether the reaction involves two $1e^-$ steps and five $2e^-$ steps. Scheme adapted from [80].

References

[1] S.K. Bhattacharya, (Ed.): Metal-filled polymers (properties and applications). Marcel Dekker, New-York (1986).

[2] C. Kvarnström in: Electrochemical Dictionary, 2nd edn., A.J. Bard, G. Inzelt, F. Scholz, (Eds.), Springer, Heidelberg (2012), p. 151.

[3] G. Inzelt, Conducting polymers. A new era in electrochemistry, 2nd edn. in: Monographs in electrochemistry, F. Scholz (Ed.), Springer, Berlin Heidelberg, (2012).

[4] U. Lang, N. Naujoks, J. Dual, Synthetic Met **159** (2009) 473.

[5] G. Inzelt, in Electroanalytical chemistry, vol. 18. A.J. Bard (Ed.), Marcel Dekker, New York (1994).

[6] G.F. Wang, X.M. Tao, R.X. Wang, Nanotechnology **19** (2008) 145201.

[7] G. Inzelt, A. Pineri, J.W. Schultze, M.A. Vorotyntsev, Electrochim. Acta **45** (2000) 2403.

[8] M.R. Lilliedala, A.J. Medforda, M.V. Madsena, K. Norrmana, F.C. Krebs, *Sol. Energ. Mat. Sol. C.* **94** (2010) 2018.

[9] E. Nasybulin, S. Wei, M. Cox, I. Kymissis, K. Levon, J. Phys. Chem. C **115** (2011) 4307.

[10] J.C. Scott, Science **304** (2004) 62.

[11] S. Möller, C. Perlov, W. Jackson, C. Taussig, S.R. Forrest, Nature **426** (2003) 166.

[12] X. Cui, D.C. Martin, Sensor. Actuat. B-Chem. **89** (2003) 92.

[13] M. Vázquez, P. Danielsson, J. Bobacka, A. Lewenstam, A. Ivaska, Sensor. Actuat. B-Chem. **97** (2004) 182.

[14] J. Bobacka, Anal. Chem. **71** (1999) 4932.

[15] J.F. Drillet, R. Dittmeyer, K. Jüttner, L. Li, K.M. Mangold, Fuel Cells **6** (2006) 432.

[16] J.F. Drillet, R. Dittmeyer, K. Jüttner, J. Appl. Electrochem. **37** (2007) 1219.

[17] C. Kvarnström, Poly(thiophene), in: Electrochemical Dictionary, 2nd edn., A.J. Bard, G. Inzelt, F. Scholz (Eds.), Springer, Heidelberg (2012).

[18] J. Bobacka, A. Lewenstam, A. Ivaska, J. Electroanal. Chem. **489** (2000) 17.

[19] H. Yamato, M. Ohwa, W. Wernet, J. Electroanal. Chem. **397** (1995) 163.

[20] N. Sakmeche, S. Aeiyach, J.J. Aaron, M. Jouini, J.C. Lacroix, P.C. Lacaze, Langmuir **15** (1999) 2566.

[21] A. Zykwinska, W. Domagala, B. Pilawa, M. Lapkowski, Electrochim. Acta **50** (2005) 1625.

[22] M. Ujvári, M. Takács, S. Vesztergom, F. Bazsó, F. Ujhelyi, G.G. Láng, J. Solid. State. Electrochem. **15** (2011) 2341.

[23] G.G. Láng, M. Ujvári, F. Bazsó, S. Vesztergom, F. Ujhelyi, Electrochim. Acta **73** (2012) 59.

[24] M. Ujvari, J. Gubicza, V. Kondratiev, K.J. Szekeres, G.G. Láng, J. Solid. State. Electrochem., **19** (2015) 1247.

[25] M. Ujvari, G.G. Láng, S. Vesztergom, K.J. Szekeres, N. Kovács, J. Gubicza, J. Electrochem. Sci. Eng., article in press, doi: 10.5599/jese.225, available from world wide web: http://www.jese-online.org/

[26] G.G. Láng, C. Barbero, Laser techniques for the study of electrode processes, in: Monographs in electrochemistry, F. Scholz (Ed.), Springer, Berlin Heidelberg (2012).

[27] N. Kovács, M. Ujvári, G.G. Láng, P. Broekmann, S. Vesztergom, Instrum. Sci. Technol. **43** (2015) 633.

[28] J. Li, X-Q. Lin, Sens. Actuators B **124** (2007) 486.

[29] D.C. Martin, J. Wu, C.M. Shaw, Z. King, S.A. Spanninga, S. Richardson-Burns, J. Hendricks, J. Yang, Polym. Rev. **50** (2010) 340.

[30] Z. Zhuang, J. Li, R. Xu, D. Xiao, Int. J. Electrochem. Sci. **6** (2011) 2149.

[31] M. Irimia-Vladu, Chem. Soc. Rev. **43** (2014) 588.

[32] M.R. Majidi, A. Jouyban, K. Asadpour-Zeynali, Electrochim. Acta **52** (2007) 6248.

[33] X. Tu, Q. Xie, S. Jiang, S. Yao, Biosens. Bioelectron. **22** (2007) 2819.

[34] J. Wen, L. Zhou, L. Jin, X. Cao, B.-C. Ye, J. Chromatogr. B **877** (2009) 1793.

[35] Y. Li, P. Wang, L. Wang, X. Lin, Biosens. Bioelectron. **22** (2007) 3120.

[36] A. Boateng, F. Iraque, A. Brajter-Toth, Electroanalysis **25** (2013) 345.

[37] T.A. Bendikov, T.C. Harmon, Anal. Chim. Acta **551** (2005) 30.

[38] J.-M. Lin, Y.-L. Su, W.-T. Chang, W.-Y. Su, S.-H. Cheng, Electrochim. Acta **149** (2014) 65.

[39] A. Boateng, R. Cohen-Shohet, A. Brajter-Toth, Electrochim. Acta **56** (2011) 7651.

[40] A. Elschner, PEDOT : principles and applications of an intrinsically conductive polymer, CRC Press, Boca Raton (2011).

[41] G.A. Snook, C. Peng, D.J. Fray, G.Z. Chen, Electrochem. Comm. **9** (2007) 83.

[42] E. Poverenov, M. Li, A. Bitler, M. Bendikov, Chem. Mater. **22** (2010) 4019.

[43] A.I. Melato, A.S. Viana, L.M. Abrantes, Electrochim. Acta, **54** (2008) 590.

[44] K. Cysewska, J. Karczewski, P. Jasiński, Electrochim. Acta, **176** (2015) 156.

[45] G.C. Arteaga, M.A. del Valle, M. Antilen, F.R. Diaz, M.A. Gacitua, P.P. Zamora, J.C. Bernede, L. Cattin, G. Louarn, Int. J. Electrochem. Sci. **7** (2012) 7840.

[46] R. Kiefer, G.A. Bowmaker, P.A. Kilmartin, J. Travas-Sejdic, Electrochim. Acta, **55** (2010) 681.

[47] Z.A. King, C.M. Shaw, S.A. Spanninga, D.C. Martin, Polymer **52** (2011) 1302.

[48] E. Nasybulin, S. Wei, I. Kymissis, K. Levon, Electrochim. Acta, **78** (2012) 638.

[49] T.E. Moustafid, R.V. Gregory, K.R. Brenneman, P.M. Lessner, Synt. Met., **135–136** (2003) 435.

[50] B. Zanfrognini, A. Colina, A. Heras, C. Zanardi, R. Seeber, J. López-Palacios, Polym. Degrad. Stabil. **96** (2011) 2112.

[51] X. Du, Z. Wang, Electrochim. Acta **48** (2003) 1713.

[52] L. Pigani, A. Heras, A. Colina, R. Seeber, J. Lopez-Palacios, Electrochem. Commun. **6** (2004) 1192.

[53] E. Ventosa, A. Colina, A. Heras, A. Martínez, O. Orcajo, V. Ruiz, J. López-Palacios, Electrochim. Acta **53** (2008) 4219.

[54] S. Lupu, F.J. del Campo, F.X. Muñoz, J. Electroanal. Chem. **687** (2012) 71.

[55] C. Zhou, Z. Liu, X. Du, S.P. Ringer, Synt. Met. **160** (2010) 1636.

[56] G. Inzelt, G.G. Láng: Electrochemical Impedance Spectroscopy (EIS) for Polymer Characterization, in Electropolymerization: Concepts, Materials and Applications, S. Cosnier and A. Karyakin (Eds.), Chapter 3, Wiley-VCH Verlag GmbH & Co. KGaA, Weinheim (2010).

[57] L.F.Q.P. Marchesi, F.R. Simoes, L.A. Pocrifka, E.C. Pereira, J. Phys. Chem. B **115** (2011) 9570.

[58] Q. Pei, O. Inganaes, J. Phys. Chem. **96** (1992) 10507.

[59] Q. Pei, O. Inganaes, J. Phys. Chem. **97** (1993) 6034.

[60] V. Tabard-Cossa, M. Godin, P. Grütter, I. Burgess, R.B. Lennox, J. Phys Chem. B **109** (2005) 175317.

[61] G.G. Láng in: A.J. Bard, Gy. Inzelt, F. Scholz (Eds.) Electrochemical Dictionary, 2nd, Revised and Extended Edition, Springer, Heidelberg (2012), p. 59.

[62] G.G. Láng, N.S. Sas, S. Vesztergom Chem. Biochem. Eng. Q. **23** (2009) 1.

[63] K. Ueno , M. Seo, J. Electrochem. Soc. **146** (1999) 1496.

[64] S.N. Sahu, J. Scarminio, F. Decker, J. Electrochem. Soc. **137** (1990) 1150.

[65] S. Cattarin, E. Pantano, F. Decker, Electrochem. Commun. **1** (1999) 483.

[66] R. Raiteri, H-J Butt, M Grattarola, Scanning Microscopy **12** (1998) 243.

[67] O.E. Kongstein, U. Bertocci, G.R. Stafford, J. Electrochem. Soc. **152** (2005) C116.

[68] M. Godin, V. Tabard-Cossa, Y. Miyahara, T. Monga, P.J. Williams, L.Y. Beaulieu, B. Lennox, R. Bruce, P. Grütter, Nanotech. **21** (2010) 075501.

[69] G.G. Láng, M. Seo, K.E. Heusler, J. Solid State Electrochem. **9** (2005) 347.

[70] G.G. Stoney, Proc Roy. Soc. London **A32** (1909) 172.

[71] G.G. Láng, K. Ueno, M. Ujvári, M. Seo, J. Phys. Chem. B **104** (2000) 2785.

[72] G.G. Láng, M. Seo, J. Electroanal. Chem. **490** (2000) 98.

[73] G.G. Láng, J. Appl. Phys. **107** (2010) 116104-1.

[74] J. Wu, Morphology of Poly(3,4-ethylene dioxythiophene) (PEDOT) Thin Films, Crystals, Cubic Phases, Fibers and Tubes, PhD Thesis, The University of Michigan (2011).

[75] T. Takano, H. Masunaga, A. Fujiwara, H. Okuzaki, T. Sasaki, Macromolecules **45** (2012) 3859.

[76] Zh. Qi, N.G. Rees, P.G. Pickup, Chem. Mater. **8** (1996) 701.

[77] P. Soudan, Ph. Lucas, L. Breau, D. Bélanger, Langmuir **16** (2000) 4362.

[78] P. Tehrani, A. Kanciurzewska, X. Crispin, N.D. Robinson, M. Fahlman, M. Berggren, Solid State Ionics **177** (2007) 3521.

[79] H. Harada, T. Fuchigami, Ts. Nonaka, J. Electroanal. Chem. **303** (1991) 139.

[80] U. Barsch, F. Beck, Electrochim. Acta **41** (1996) 1761.

[81] X. Crispin, S. Marciniak, W. Osikowicz, G. Zotti, A.W. Denier van der Gon, F. Louwet, M. Fahlman, L. Groenendaal, F. de Schryver, W.R. Salaneck, J. Polymer Sci. B **41** (2003) 2561.

[82] S. Marciniak, X. Crispin, K. Uvdal, M. Trzcinski, J. Birgerson, L. Groenendaal, F. Louwet, W.R. Salaneck, Synt. Met. **141** (2004) 67.

[83] A. Elschner, Sol. Energ. Mat. Sol. Cells **95** (2011) 1333.

[84] F. Mohammad, P.D.Calvert, N.C. Billingham, Synt. Met. **66** (1994) 33.

[85] P. Rannou, M.Nechtschein, Synt. Met. **101** (1999) 474.